Colloid Polym Sci 279:203–213 (2001)

ORIGINAL CONTIBUTION

E. M. Antipov
A. A. Levchenko
M. Stamm
P. J. Lemstra

Structure and temperature behavior of thermotropic liquid-crystalline Ultrax copolyesters

Received: 20 July 1999
Accepted: 20 August 2000

E. M. Antipov · A. A. Levchenko
Topchiev Institute of Petrochemical Synthesis, Russian Academy of Sciences
Leninsky pr. 29, 117912 Moscow, Russia

M. Stamm (✉)
Institut für Polymerforschung Dresden e.V., Hohe Strasse 6
01069 Dresden, Germany
e-mail: stamm@ipfdd.de
Tel.: +49-351-4658224
Fax: +49-351-4658281

P. J. Lemstra
Eindhoven University of Technology
Polymer Chemistry and Technology
Center for Polymers and Composites
5600 MB Eindhoven, The Netherlands

Abstract Phase and relaxational transitions in the commercial thermotropic liquid-crystalline copolyesters Ultrax 4002 and Ultrax 4003 were studied by X-ray diffraction, differential scanning calorimetry, and mechanical analysis. In spite of only a slight difference in the compositions of the copolyesters, considerable differences in their structure and temperature behavior were observed. In particular, it was shown that the degree of crystallinity differs by more than a factor of 2 for the as-spun fibers upon annealing above the glass-transition temperature. The type of crystalline structure as well as the ability to crystallize are also different. The glass-transition temperature of both copolyesters is determined as the temperature of the appearance of mobility of the most rigid comonomer units and does not depend on the composition of the materials. Annealed copolyesters are semicrystalline materials with a two-phase structure, where the crystalline phase coexists with a liquid-crystalline one. The structure of the latter is characterized by aperiodic positions of smecticlike layers in space. On heating the materials the crystalline phase is transformed into a pseudo-hexagonal mesophase indicating features of a second-order phase transition.

Key words X-ray diffraction · Thermotropic liquid-crystalline copolyesters · Highly oriented fibers · Two-phase composition · Aperiodic smecticlike structure

Introduction

Thermotropic liquid-crystalline (LC) polyesters have been of considerable interest both scientifically and commercially because of their excellent mechanical properties, thermal stabilities, chemical and flame resistance, and especially of the ease in producing uniform molecular orientation under elongational flow, resulting in a low melt viscosity along the flow direction and giving rise to high strength fibers by melt extrusion [1].

The considerable academic interest results, first of all, from the ability of these materials (they are, as a rule, random copolymers with a statistical distribution of comonomer units within macromolecules) to crystallize in any combination and ratios of their components [2]. Two principally different models have been proposed to describe the solid-state structure of these copolymers. The nonperiodic layer model by Windle et al. [3] agrees very well with morphological studies, but cannot describe satisfactorily the wide-angle X-ray scattering (WAXS) diffractograms. The paracrystalline model by Guttierezz et al. [4] shows good agreement with the experimental X-ray patterns, but the molecular picture behind the model is not very plausible. It is expected that perhaps a combination of elements of both models may in the future give a more realistic physical picture of the structure of random LC copolyesters (CPE).

The objective of our study largely concerns the determination of the structure of the noncrystalline phase component of such materials. Indeed, if CPEs are

able to crystallize, they should be semicrystalline polymers. It is essential to note that their crystallinities seldom exceed 30%. Taking into account the rigid nature of the comonomer units, the question of the structure of the noncrystalline phase is puzzling. Our experience in this field shows that the structure of the noncrystalline phase happens to be unusual and interesting [5–9].

From the ability of stiff-chain CPEs to form thermotropic LC structures [1], one can expect that the development of LC nematic phases is most probable in these materials. However, in addition to nematic states smecticlike structures were also recently found for some CPEs [5–9]. New mesophases form either a periodic layer structure typical for smectics or an unusual aperiodic one. The development of the smectic LC structure is already an interesting observation by itself, since those macromolecules do not contain physically pronounced mesogenic groups within main or side chains. The aperiodic smectic structures, never observed for polymers before, are not only stable within a wide temperature range, but also exist up to [5–9] and even above [10] the melting point of the crystalline phase.

Thus, our general interest is to realize whether such structures are inherit only of some special representatives of the class of thermotropic LC CPEs, or if they are characteristic of all such materials. In addition to the data presented earlier [5–9], we report the results of the study of one further family of thermotropic LC random CPEs, so-called Ultrax, which are commercial products.

Experimental

The three-component wholly aromatic CPEs Ultrax 4002 (CPE-1) and Ultrax 4003 (CPE-2) produced by BASF, Ludwigshafen, Germany, were prepared from terephthalic acid, isophthalic acid, and *p*,*p*-dioxybiphenol. The specimens and the data on their compositions were kindly provided by V.G. Kulichikhin (Topchiev Institute of Petrochemical Synthesis, Moscow, Russia). The compositions were obtained from IR investigations. According to these data, the CPEs have the chemical structure shown in Fig. 1.

CPE fibers were prepared by melt extrusion at 350 °C using a Brabender rheoscope. The diameter of the monofilaments was typically 10 μm. Both as-spun fibers and those subject to prolonged multistep annealing (10.5 h at 192 °C, 8 h at 212 °C, and 8 h at 235 °C) were studied. The annealing conditions were chosen on the basis of differential scanning calorimetry (DSC) and mechanical data. Specimens for X-ray analysis were prepared by stacking about 300 monofilaments aligned in parallel to a compact bundle. Measurements of temperature dependence were carried out under isometric conditions (ends of fibers were fixed). For DSC measurements we used 10–20 mg sample material placed in sealed standard pans. To avoid thermal prehistory, each sample was used only once.

X-ray diffraction studies were carried out with a standard Siemens D 500T θ–θ diffractometer using copper radiation. The beam was monochromatized with a graphite crystal ($\lambda = 0.154$ nm). Equatorial and meridional diffraction patterns were recorded in transmission mode using a scintillation counter as a detector. Slit collimation of the primary and diffracted beams was used. In addition, we used a pulse-height descriminator adjusted to Cu Kα radiation. The temperature of measurements was varied from 20 to 300 °C.

Two dimensional WAXS and small-angle X-ray scattering (SAXS) patterns were registered with an 18-kW Rigaku X-ray generator. The rotating anode was used as a source of copper radiation. The primary beam, 0.5 mm in diameter, was monochromatized with two graphite crystals ($\lambda = 0.154$ nm). A two-dimensional gas detector (Siemens) was used to record patterns in transmission mode with a specimen placed in a special chamber under vacuum. By changing the sample-to-detector distance either WAXS or SAXS patterns were obtained. The maximum length of the optical bench was 3 m. The typical exposure time was up to 10 h. Measurements were carried out at ambient temperatures.

Thermal properties of the samples were studied using a Mettler TA 4000 differential calorimeter within a temperature range extending from 20 to 350 °C at a heating or cooling rate of 20 °C/min. All DSC measurements were carried out with CPE fibers kept with free ends (nonisometric conditions).

Dynamic viscoelastic characteristics of CPE fibers were measured using the Rheometrix instrument at frequencies 1, 10, and 100 Hz and temperatures 20, 100, and 150 °C. The amplitudes of dynamic loading did not exceed the region of linear viscoelasticity. Different levels of loading corresponding to different degrees of extension were used. Standard mechanical tests and shrinkage measurements were performed using an Instron-1121 machine equipped with a temperature chamber.

Results and discussion

Analysis of DSC data and results of mechanical tests

CPE-1 and CPE-2 samples were first analyzed with respect to their thermal behavior. DSC traces during

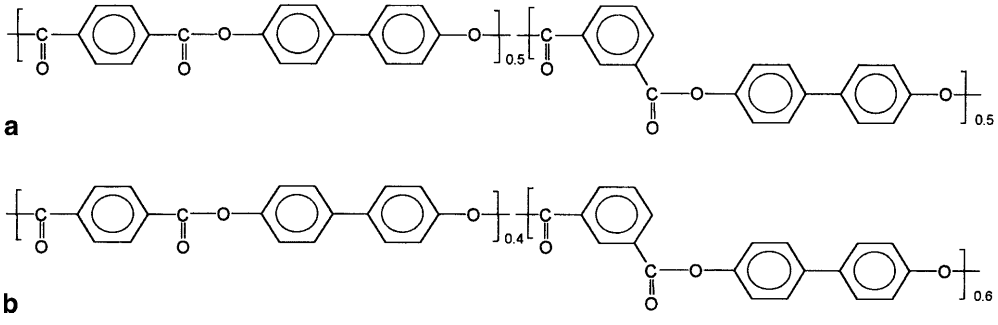

Fig. 1 The chemical structure of **a** CPE-1 and **b** CPE-2

heating, cooling, and reheating cycles of as-spun fibers of CPEs under study are shown in Fig. 2. Upon first heating of both samples a wide endothermic effect is observed extending from 140 to 300 °C for CPE-1 and from 220 to 340 °C for CPE-2. On cooling from the temperature of extrusion (350 °C), where the viscosity of the materials is very low, in the DSC trace of the first sample a steplike change of the curve typical of a glass transition is observed in the temperature range 110–140 °C. The glass-transition temperature estimated from the inflection point is 124 °C. On reheating CPE-1 the glass transition (119–133 °C) is again well pronounced and the inflection point is localized at 126 °C. Thus, the glass-transition temperature is determined to be approximately 125 °C.

In contrast to CPE-1, the glass transition is not detectable in the DSC traces of as-spun CPE-2 fibers, indicating perhaps a relatively small content of the noncrystalline phase in the material. Indeed, in the DSC trace of the cooling cycle one can recognize only a weak exothermic maximum localized between 305 and 265 °C,

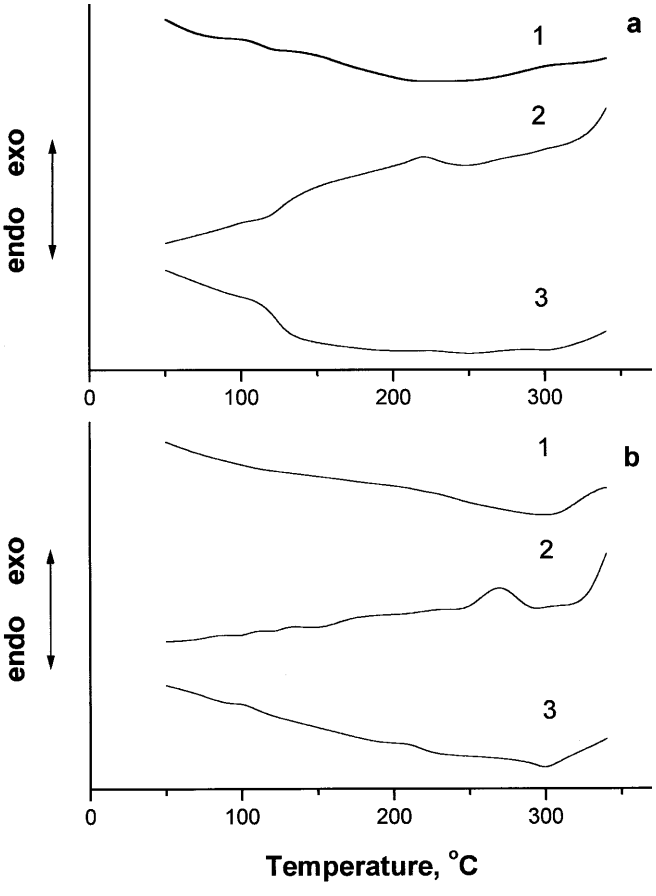

Fig. 2 Differential scanning calorimetry traces registered on heating (*1*), cooling (*2*), and reheating (*3*) of as-spun fibers of **a** CPE-1 and **b** CPE-2

whereas on reheating, the DSC trace exhibits a corresponding endothermic effect extending from 265 to 320 °C. Such hysteresis of thermal effects during heating–cooling cycles is a common feature of the first-order phase transition in semicrystalline polymers. Thus, it is rather probable that CPE-2 is a crystalline polymer containing a relatively high amount of the ordered phase already in the initial fibers.

It has been reported previously [11] that the glass-transition range of CPE-2 is similar to that of CPE-1 and coincides with the temperature of defreezing of the local mobility of the most thermally stable comonomer unit in the CPE material, namely, the biphenol group. Such a coincidence appears to be a universal feature of all thermotropic LC CPEs [12]; however, in our case it is essential to note that a relatively small difference in the composition of the CPEs under study leads to a considerable change in the temperature behavior.

In addition to the DSC examination, the monofilaments of the CPEs were studied by dynamic mechanical analysis by varying the initial loading of the sample, the temperature, and the frequency of the loading–unloading cycles. To begin with, measurements were carried out over 15 min in order to obtain an estimate of the dynamic modulus.

The experimental data obtained at ambient temperature and a frequency of 10 Hz are shown in Fig. 3. It was found that the character of the curves is also similar for other experimental conditions. Qualitatively the dependences presented are typical of all LC polymers [13]. The main quantitative difference between the CPEs under study is related to the nearly threefold higher modulus of the CPE-2 fibers than of the CPE-1 ones. This fact might again indicate a different level of crystallinity in the two CPEs.

Figure 3 shows that the modulus E' increases with increasing force applied to both materials. Upon unloading the value is always higher than upon first loading, indicating an increase in rigidity of the CPE fibers. For all the following cycles the loading–unloading curves coincide with the unloading one in the first cycle.

The results of static examination of the samples agree well with the data of the dynamic mechanical tests. The stress–strain plots recorded at room temperature for both CPEs (not shown here) have the typical form of uniform convex curves and indicate a decrease in the modulus when the stress rises. Again corresponding estimations show that the value of the modulus for the CPE-1 fibers (20 GPa) is approximately 3 times smaller than that for the CPE-2 material (60 GPa). At elevated temperatures, the character of the deformation behavior for both CPEs remains almost the same. Only the elongation at break, being similar for both materials at ambient temperatures, differs at 150 °C: it is 2.8 and 5.0% for CPE-1 and CPE-2, respectively.

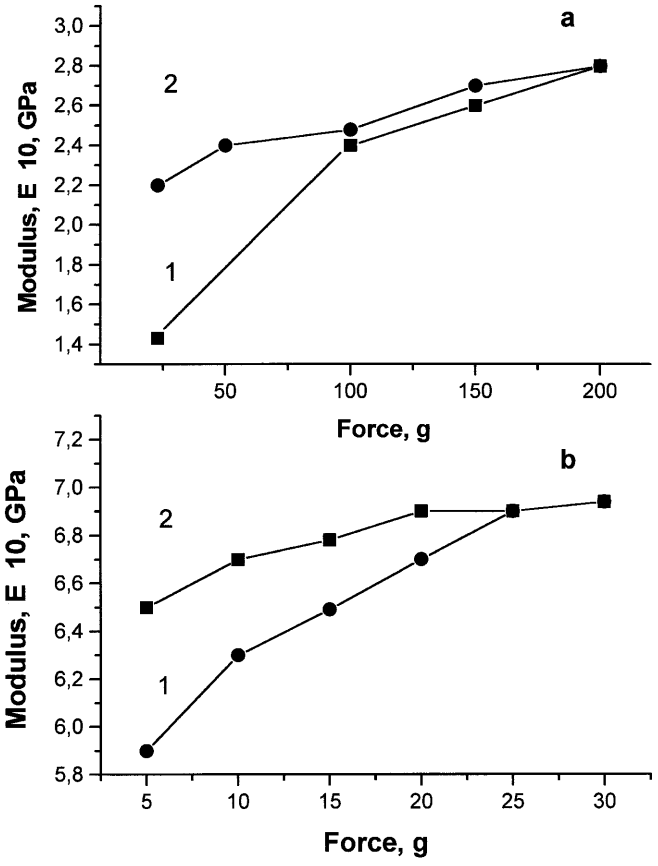

Fig. 3 Dynamic mechanical data for as-spun fibers of **a** CPE-1 and **b** CPE-2 registered on first loading (*curve 1*) and unloading (*curve 2*)

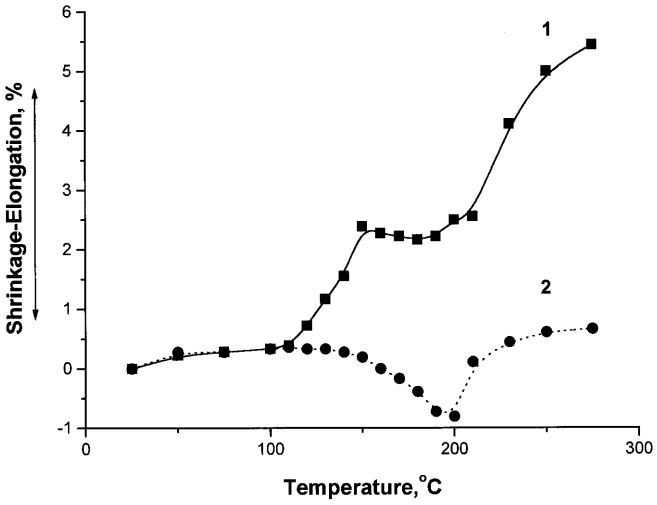

Fig. 4 Temperature dependences of elongation–shrinkage measurements on heating of as-spun fibers of CPE-1 (*curve 1*) and CPE-2 (*curve 2*)

A more complicated discrepancy is observed when shrinkage is measured during heating of as-spun CPE fibers (Fig. 4). As one can expect, up to 100 °C the length of the CPE-1 fibers hardly changes. On further heating to the glass-transition range (100–150 °C), a considerable elongation of the sample is observed followed by stabilization of the sample's dimensions at higher temperatures (150–180 °C), and subsequently, by a secondary elongation range above 180 °C.

The situation looks like the competition between two processes of opposite direction which take place in the material. According to our data [13] heating as-spun fibers of stiff-chain LC polymers above the glass-transition temperature usually leads to an increase in the degree of orientation of the stiff macromolecules accompanied by an elongation of the length of the sample on the whole. In the case of CPE-1 such a behavior is observed upon heating from 100 to 150 °C (Fig. 4, curve 1). Then, or in parallel, another process starts to act, probably related to the crystallization of the material, which is usually accompanied by a shrinkage due to the development of a more perfect structure. Indeed, the plateaulike part of the curve is observed between 150 and 180 °C. It seems probable that the crystallization is completed at 180 °C, and on further heating the secondary elongation process becomes predominant. It may indicate a complicated character of the high-temperature evolution of the structure. It is essential to note that according to the data of dynamic mechanical tests, the material starts to flow at 180 °C; however, one cannot see any indication of melting in the DSC curve in this range of temperatures (Fig. 2a).

The temperature behavior of the CPE-2 fibers (Fig. 4, curve 2) rather differs from that for the first CPE. Before the glass-transition temperature the length of the sample remains stable followed by a shrinkage within the range 125–180 °C and, then, by an elongation of the sample as observed for CPE-1. If one takes into account that the content of the crystalline phase in the initial material may be higher than for CPE-1, it might be expected to find the absence of elongation during heating of the sample above the glass-transition temperature. The network of crystallites and the low mobility prevent the process of additional orientation of chains on heating leading to stable dimensions of fibers in this temperature region. Above 125 °C only recrystallization may start, resulting in the shrinkage of the sample on heating up to 180 °C followed by secondary elongation as was also observed for CPE-1. We should note that in contrast to CPE-1, the CPE-2 material only starts to flow at 270 °C (instead of 180 °C for CPE-1).

In order to identify the complicated sequence of phase and relaxation transitions on heating both copolymers under study, X-ray analysis at ambient and elevated temperatures was carried out.

Structure and phase composition of as-spun and annealed CPE fibers from X-ray analysis

Taking into account the data of DSC and mechanical analysis, one can identify the following temperature regions to be of most interest: the temperature range up to 100 °C; the region centered at 125 °C; the range between 150 and 180 °C; and, finally, the high-temperature region extending above 180 °C. Note that the annealing regime of as-spun CPE fibers (see Experimental) was chosen namely within the latter temperature range, where as shown earlier [11] the highest degree of crystallinity of the materials was reached.

To begin with the first temperature range the structure of as-spun and annealed CPE fibers at room temperature was investigated. Two-dimensional WAXS and SAXS patterns of as-spun fibers of both CPEs (Fig. 5a, b) reveal the high degree of chain orientation. One can also see that the assumption proposed earlier is really true: in contrast to CPE-1, the initial CPE-2 fibers already contain a large amount of the crystalline phase. The existence of well-pronounced Bragg reflections not only in the equator and meridian but also in the quadrants of the X-ray pattern, in particular in the first layer line (Fig. 5b), well proves this conclusion.

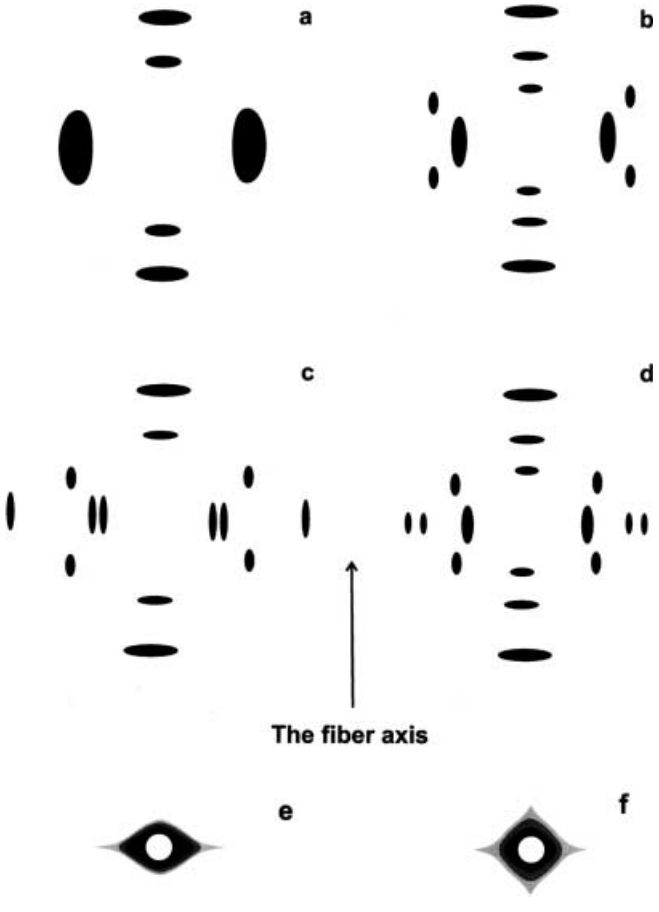

Fig. 5 Schematic representation of wide-angle X-ray scattering (*a–d*) and small-angle X-ray scattering (*e*, *f*) patterns of as-spun (*a*, *b*, *e*) and annealed (*c*, *d*, *f*) fibers of CPE-1 (*a*, *c*, *e*, *f*) and CPE-2 (*b*, *d*) obtained at ambient temperature. The fiber axis is vertical

As may be expected, annealing leads to the development of crystallinity in both materials (Fig. 5c, d). The analysis of X-ray patterns of annealed fibers shows considerable differences in the crystalline structure of the two CPEs. In particular, the main reflection in the equator in the case of CPE-1 has a double character, whereas only one Bragg spot is observed almost at the same angular position in the equator of the CPE-2 X-ray pattern. In addition, in the case of CPE-2 the meridional maximum in the second layer line is observed, whereas for the first CPE it is absent there, etc. These facts indicate different types of crystalline modifications developed upon annealing of the CPEs under study. Again one may be surprised that such a slight difference in the chemical structure leads to considerable changes in the crystalline structures.

SAXS patterns of as-spun and annealed fibers of both CPEs are typical of those of other representatives of this class of copolymers [6–8]. Because the SAXS patterns of both copolymers are similar, they are shown in Fig. 5e and f for only one of them. According to the analysis carried out in Ref. [14], the weak diffuse scattering observed in the meridian of the SAXS patterns goes along with the absence of long periodicity, while the relatively intensive diffuse scattering in the equator indicates a well-developed porosity of the materials. It was shown [14] that the long axes of such anisotropic microvoids are parallel to the fiber direction, whereas the small axes are oriented perpendicularly. Compared with the as-spun CPE fibers (Fig. 5e), in the annealed samples not only equatorial but also meridional small-angle scattering is relatively intense (Fig. 5f). The peculiar cross-shaped form of SAXS suggests that randomly distributed microvoids in CPE fibers may have the form of parallelepipeds.

The detailed analysis of WAXS patterns was carried out on the basis of the equatorial and meridional diffraction patterns shown in Figs. 6 and 7 for as-spun and annealed fibers of CPE-1 and CPE-2, respectively.

The equatorial diffractogram of as-spun CPE-1 fibers (Fig. 6a) shows a strong diffuse maximum at $2\theta = 19.9°$. The profile reminds on the one of the thermotropic LC CPE known as Vectra [7]. The meridional scattering shows distinct Bragg reflections in the fourth ($2\theta_{004} = 28.27°$) and sixth ($2\theta_{006} = 43.76°$) layer lines, which, as the corresponding calculations show, are not exactly periodic. The analysis of such aperiodic maxima for the Vectra CPE resulted in the development of two different models of its crystalline structure mentioned before [3, 4].

However, the pseudoamorphous character of the profile of the equatorial scattering in the X-ray pattern

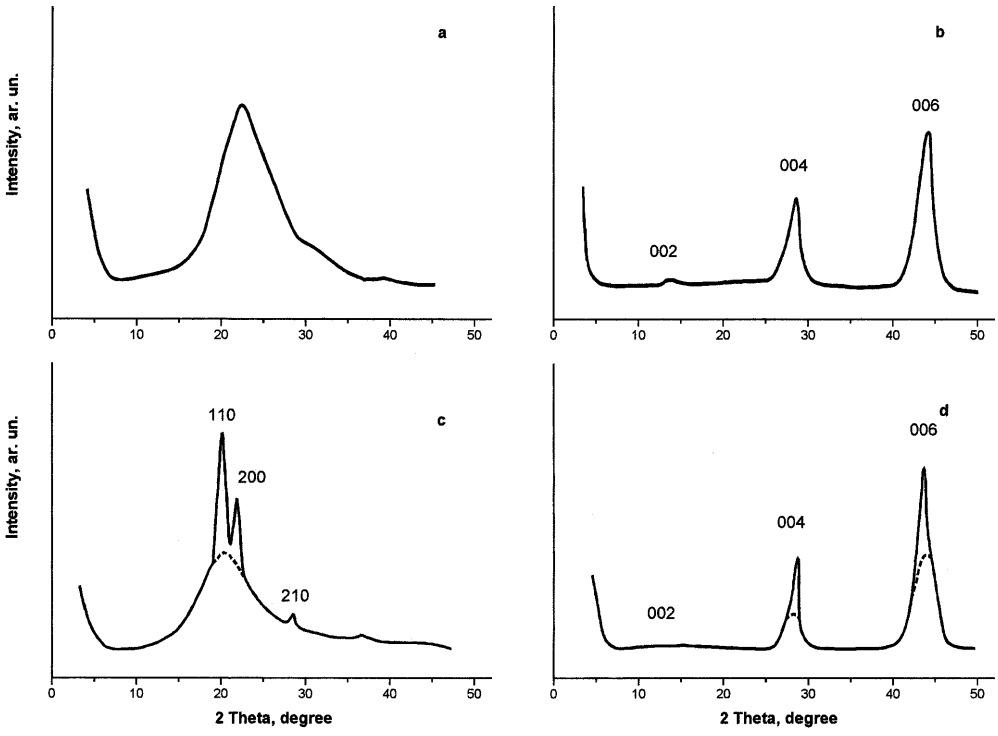

Fig. 6 Equatorial (**a**, **c**) and meridional (**b**, **d**) diffractograms of as-spun (**a**, **b**) and annealed (**c**, **d**) fibers of CPE-1 obtained at ambient temperature. The conditions of annealing are presented in the Experimental part

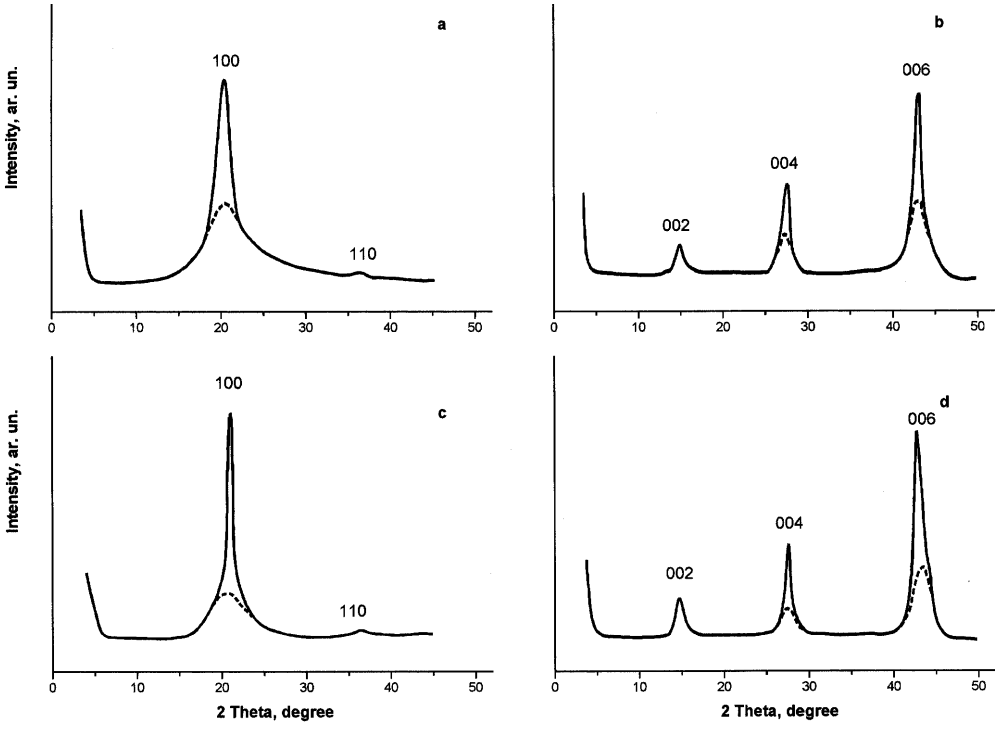

Fig. 7 Equatorial (**a**, **c**) and meridional (**b**, **d**) diffractograms of as-spun (**a**, **b**) and annealed (**c**, **d**) fibers of CPE-2 obtained at ambient temperature. The conditions of annealing are presented in the Experimental part

of CPE-1 in addition to the absence of Bragg reflections in the quadrants allows the conclusion to be drawn that there are no indications of the existence of a crystalline phase in this material. The structure of CPE-1 looks like that of a single-phase material, or at least like a system containing only a very small number (less than 5%, which is the limit of sensitivity of the method) of small crystallites (not more than 7–8 nm in size).

Detailed analysis of the data obtained for other representatives of this class of copolymers [6–8] showed that such a structure should better be identified with a LC smectic phase with nonperiodic layers rather than with a crystalline phase [5, 9]. The X-ray pattern of as-spun fibers of CPE-1 also possess all the features of such a structure.

Upon annealing CPE-1 above 180 °C (see Experimental), the material crystallizes, resulting in the development of Bragg reflections in the X-ray pattern, as mentioned previously (Fig. 5c). Indeed, the appearance of a number of maxima in the equator (Fig. 6c) and in quadrants (Fig. 5c) indicates this process. In addition, one can see (Fig. 6c, d) that after annealing sample CPE-1 becomes semicrystalline, where approximately 16% of the crystalline phase coexists with the aperiodic LC smectic phase component (the procedure of the estimation of crystallinity for oriented CPE fibers is described in Ref. [14]).

Analysis of angular positions and intensities of 11 Bragg reflections in the X-ray pattern of annealed fibers of CPE-1 shows that the best fit between calculated and experimental data is obtained for an orthorhombic crystalline modification. Using a least-squares procedure we can estimate the parameters of the unit-cell: $a = 0.838$, $b = 0.528$, and $c = 1.258$ nm. The main crystallographic data are presented in Table 1.

In CPE-2, one can see (Fig. 7) that already the initial as-spun fibers contain approximately 21% of the crystalline phase. This value increases twofold for the annealed material (43%). Moreover, the corresponding more detailed analysis shows that the crystalline modification of CPE-2 differs from that of CPE-1. In particular, in the equator of the X-ray pattern of as-spun and annealed fibers (Fig. 7a, c) one can see very strong (at 20.12°) and very weak (at 35.6°) reflections, whose spacings are related by a factor of 1.75. This value is very closed to the square root of 3, indicating a hexagonal type of crystalline structure in this material.

For CPE-2 the parameters of the unit cell of the crystalline modification were calculated using a set of nine Bragg reflections: $a = 0.510$ and $c = 1.205$ nm. The main crystallographic parameters are listed in Table 1. Thus, the structure of the second CPE under study is also biphasic in both as-spun and annealed fibers, where 21–43% of the crystalline phase coexists with the aperiodic LC smectic phase component.

Again, as mentioned in the previous sections, one can recognize that only a slight difference in the compositions of the CPEs under study leads to a considerable difference in the ability of the materials to crystallize. Indeed, different crystallinities are reached after annealing at similar conditions and different types of crystalline modifications are formed for the two samples.

X-ray analysis of CPE fibers at elevated temperatures

In the following we compare the evolution of the X-ray diffraction patterns registered at elevated temperatures during step-by-step heating of as-spun CPE fibers with the DSC and mechanical analysis data. The equatorial X-ray diffractograms recorded on heating fibers of CPE-1 and CPE-2 are shown in Figs. 8 and 9, respectively. In addition, the temperature dependences of the intensities and the angular positions of the main reflections in the X-ray patterns of both samples are illustrated in Figs. 10 and 11.

Before the onset of the glass transition (100 °C) the profile of the scattering curve of CPE-1 (Fig. 8) only slightly differs from that obtained at 20 °C (Fig. 6a). Meanwhile, the intensity of the main maximum slightly increases in this temperature range followed by a stronger increase within the glass-transition range

Table 1 Some crystallographic data for annealed fibers of the copolyesters (CPEs) under study obtained from wide-angle X-ray scattering patterns patterns as described in the text

	CPE-1 (crystallinity 16%)					
	Equator				Meridian	
Miller indexes	110	200	211/210	Diffusive halo	004	006
2θ (degree)	19.81	21.25	28.02	20.0	28.39	43.45
d (nm)	0.448	0.418	0.318	0.443	0.314	0.208
Half-width (degree)	0.6	0.7	–	6.0	1.2	1.5
Crystallite dimension (nm)	14.0	13.2	–	–	–	–
	CPE-2 (crystallinity 43%)					
	Equator				Meridian	
Miller indexes	100	110	Diffusive halo	002	004	006
2θ (degree)	20.12	35.6	20.42	14.83	28.04	43.29
d (nm)	0.441	0.252	0.435	0.597	0.318	0.209
Half-width (degree)	0.6	–	3	1.0	1.3	1.5
Crystallite dimension (nm)	14.0	–	–	–	–	

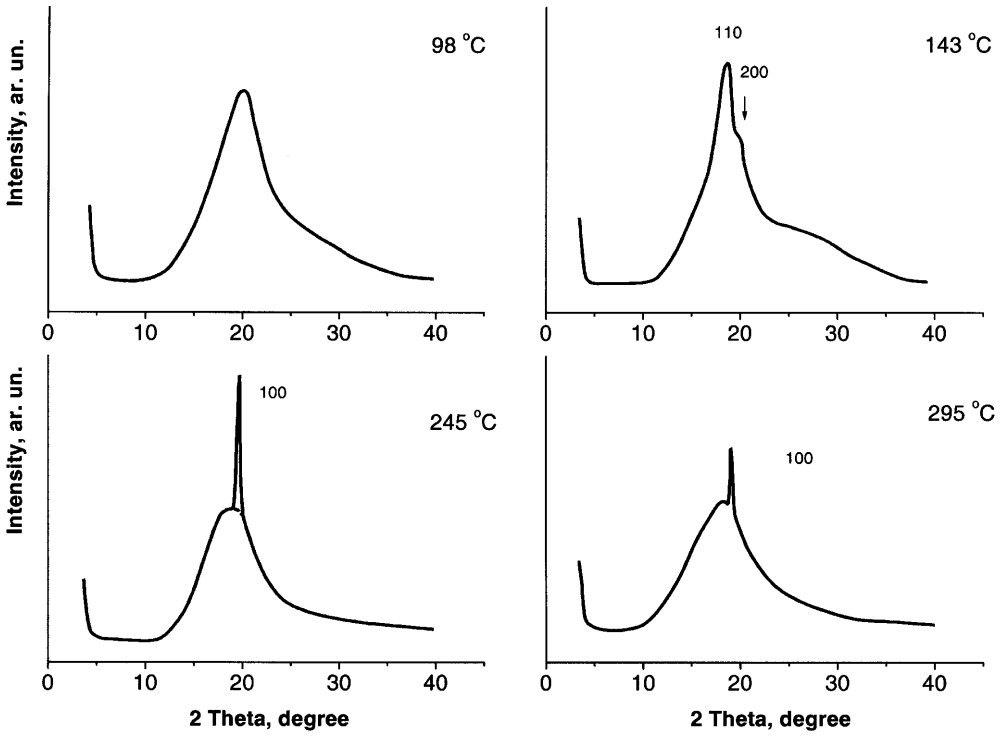

Fig. 8 Equatorial diffractograms of as-spun fibers of CPE-1 registered during multistep heating of the material at different temperatures. The time of the measurement at each temperature was 1.5 h

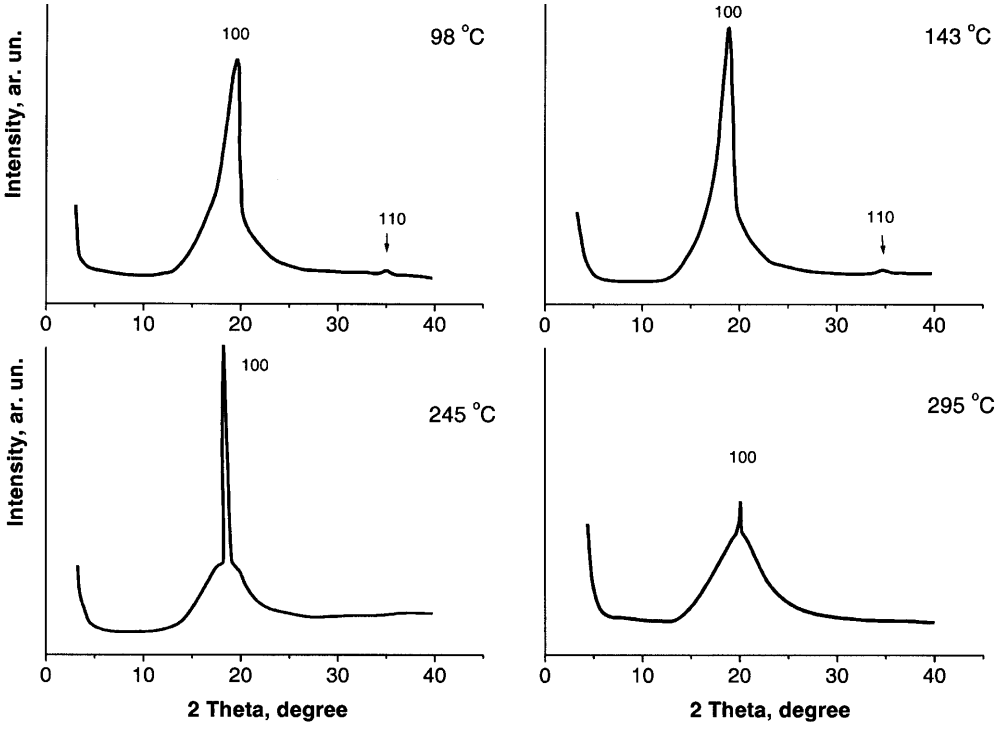

Fig. 9 Equatorial diffractograms of as-spun fibers of CPE-2 registered during multistep heating of the material at different temperatures. The time of the measurement at each temperature was 1.5 h

(100–150 °C). Such behavior correlates well with the data of the shrinkage measurements (Fig. 4, curve 1).

On further heating from 100 to 150 °C, the increase in intensity becomes nonreversible, indicating that crystallization starts to develop in parallel to thermal expansion. Indeed, the development of two Bragg reflections, (110) and (200), in the diffractogram (Fig. 8), corresponding to the orthorhombic modification of

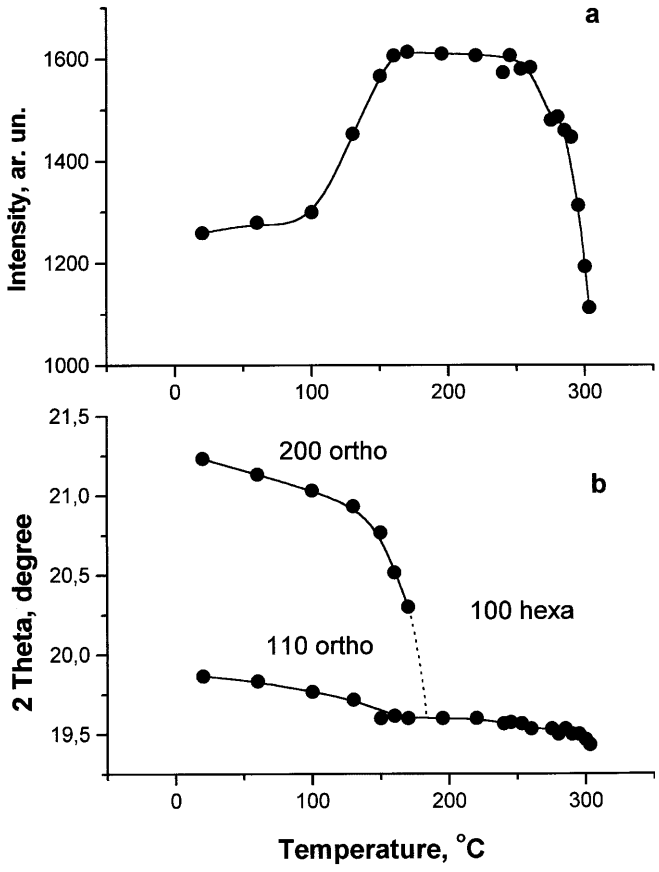

Fig. 10 Temperature dependence of the angular position of the main equatorial reflections in the X-ray pattern of as-spun fibers of CPE-1. The points for the (200_{ortho}) reflection are plotted using the data for annealed fibers. The *lines* are a guide for the eye

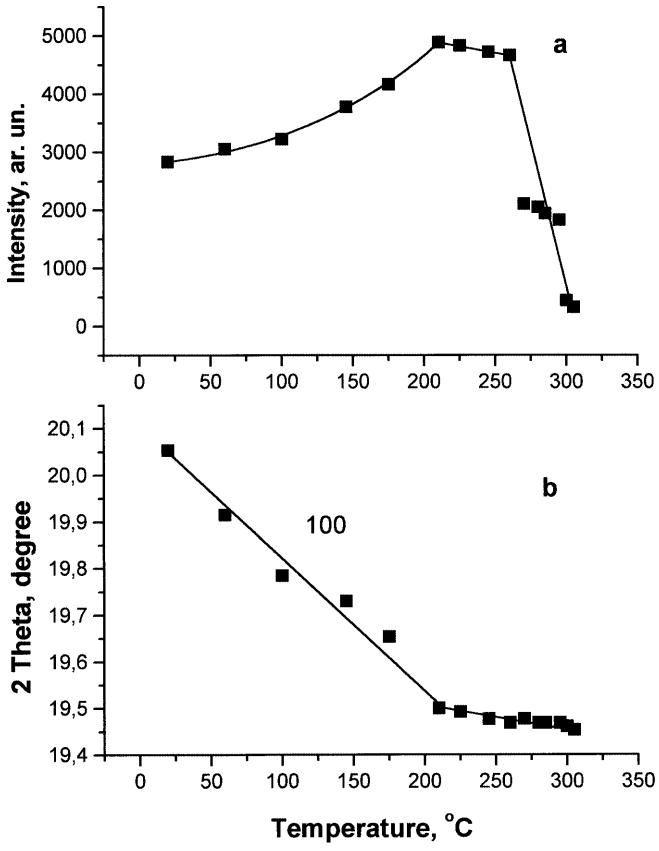

Fig. 11 Temperature dependence of the angular position of the main equatorial reflection in the X-ray pattern of as-spun fibers of CPE-2. The *lines* are a guide for the eye

crystalline CPE-1, is observed. On cooling the sample from any temperature within the range 150–180 °C, the X-ray pattern recorded at 20 °C will be almost similar to that registered at elevated temperatures and will look approximately like that shown in Fig. 6c for the annealed and subsequently cooled sample.

On heating the sample to 180 °C both main reflections of the orthorhombic modification start to overlap (Fig. 10b) owing to different slopes of the temperature dependences of the angular positions and, finally, coincide at 180–200 °C. As a result, only one strong Bragg maximum is present in the equator of the X-ray pattern (Fig. 8) superimposed on the background of the diffuse halo. Its half-width (0.4°) becomes even smaller than that for the annealed sample (Table 1), corresponding to a lateral dimension of coherently scattering regions of about 22.5 nm.

According to Ref. [15] the existence of only one narrow and intensive Bragg reflection in the equator of the X-ray pattern of CPE-1 above 180 °C is related to the development of random shifts of the chains against each other along the longitudinal direction at such high temperatures and, in addition, perhaps due to the appearance of conformational distortions in macromolecules. Such behavior is typical of mesophase structures of flexible-chain polymers known either as condis-crystalline [16] or columnar [17] mesomorphic states. This type of structure, as a rule, is characterized by two-dimensional pseudohexagonal packing of the chain centers of gravity within the plane perpendicular to the macromolecular axis. It seems probable that the high-temperature form of the structure of CPE-1 is a mesophase of this type. In other words, on heating the first CPE in the vicinity of 180 °C the phase transition from the orthorhombic crystalline to the pseudohexagonal mesomorphous state takes place.

It is well known that a mesophase of this kind possesses an increased mobility of the chain segments (compared with a crystalline phase) [16, 18]. Perhaps for to this reason the secondary elongation of the sample is observed in Fig. 4 (curve 1) to start at 180 °C, when the crystal–mesophase transition is completed. In addition, exactly at the temperature of the phase transition, the material of as-spun fibers starts to flow as mentioned

earlier. Such behavior is rather more characteristic of a mesophase structure than of a crystalline one. It is essential to note that, in contrast to the as-spun fibers, the annealed material starts to flow much later, i.e. approximately at 260 °C, when the mesophase starts to melt. Only a slight indication of the main reflection of the mesophase is left in the equator of the X-ray pattern at 295 °C. Above 300 °C the material again has the uniphase structure of a LC nematic melt.

On cooling the CPE-1 fibers from the temperature range of the existence of the mesophase, the X-ray pattern of the sample registered at room temperature looks exactly like the one shown in Fig. 6c. This means that a reversible transition from the mesophase to the orthorhombic crystal takes place. The highest level of crystallinity (16%) is reached on cooling from 235 °C, while on cooling from, for instance, 295 °C it is only about 10%; therefore we chose not to raise the annealing temperature (see Experimental) above 235 °C.

As might be expected, the temperature evolution of the structure of CPE-2 differs from that of CPE-1. Analysis of the equatorial diffractograms recorded at elevated temperatures (Figs. 9, 11) reveals that up to 200 °C the hexagonal crystalline structure remains almost like that in the initial sample. Again, as observed for CPE-1, on heating to 200 °C the intensity of the main reflection increases. Between 125 and 200 °C the crystallinity of the material increases. In parallel, the angular position of the main reflection drops monotonically owing to thermal expansion (Fig. 11); its half-width also decreases accompanied by a corresponding increase in the crystallite dimensions from 11.0 to 14.0 nm. Finally, at 200 °C the character of the temperature dependence in Fig. 11 changes considerably, indicating the transformation of the structure of the material.

Above 200 °C in the equator of the X-ray pattern of CPE-2 the (110) reflection of the hexagonal phase disappears (Fig. 9). The (100) reflection becomes narrower (the half-width is 0.3°), indicating a further increase in the dimensions of coherent scattering regions up to 24.0 nm. It is essential to note here that on cooling the material from the temperature range 200–260 °C the half-width again becomes 0.6°. This means that the crystallite dimensions change reversibly between 14.0 and 24.0 nm during heating–cooling cycles. This effect is discussed elsewhere [18, 19] and is typical for the crystal–mesophase transition, where the mesophase is, namely, of the condis-crystalline or columnar type [16, 17].

From all these observations one has to conclude that for CPE-2, as was also shown for CPE-1, the phase transition from the hexagonal crystal to the pseudohexagonal mesophase is observed at 200 °C (while for CPE-1 it was at 180 °C). Again on cooling the material from the temperature range where the mesophase exists, the reversible sequence of the transitions takes place. The mesophase starts to melt at 270 °C (at this temperature the material also starts to flow), followed by the transition to the LC nematic melt above 320 °C. Namely, between 270 and 320 °C an endothermic effect is observed in the DSC trace of reheated CPE-2 (Fig. 2b).

To recall the discussion on the data presented in Fig. 4, the following explanation may be given for the temperature-dependent changes of the fiber dimensions. One may take into account that the initial sample of CPE-2 is already crystalline, and that the network of crystallites may prevent the elongation process on heating the sample. Thus, it is understandable that elongation is not observed above the glass-transition temperature, as it takes place for CPE-1. In contrast, a slight shrinkage of the sample due to, perhaps, some additional crystallization during annealing of the material is observed at 180–200 °C, followed by a secondary elongation process, which develops when the transition to the mesophase is complete.

Conclusions

The detailed analysis of the structure, phase composition, and temperature behavior of the two CPEs under study allows the structure of all phase components as well as of all phase and relaxational transitions on heating–cooling cycles of the materials to be identified.

It was found that only a slight change in the chemical structure of the CPEs, namely, a 5% change in the ratio of terephthalic acid to isophthalic acid content results in a considerable difference in the behavior of the material. Indeed, the structure of the initial fibers of CPE-1 is uniphase and noncrystalline, whereas the as-spun fibers of CPE-2 already contain a lot of the crystalline phase. The crystalline structure developed in CPE-1 during annealing above the glass-transition temperature is orthorhombic, while that in CPE-2 is hexagonal. Finally, the highest level of crystallinity reached by multistep annealing at elevated temperatures of the two CPEs differs by approximately a factor of 2 in the materials.

Both copolymers also exhibit features which are typical of other representatives of this class of thermotropic LC CPEs. In particular, the noncrystalline phase of the materials has the structure of so-called aperiodic LC smectics, which has been described as a new type of LC states in polymers. Upon heating both CPEs, a phase transition from the crystalline state to the pseudohexagonal mesophase is observed. This mesomorphic state is typical, as a rule, for flexible-chain polymers, where the chains do not contain mesogenic groups; however, it seems that this type of mesophase structure is also an inherent feature of the random stiff-chain CPEs.

At the very end of the discussion, only one main question remains open. What is the order of the crystal–mesophase phase transition observed in those materials? Indeed, the absence of a well-pronounced heat effect in the DSC trace, the change in the slope (instead of a steplike drop) observed in the temperature dependences of angular positions of crystalline reflections (or, alternatively, in the corresponding temperature dependences of the spacings), and the reversible character of the structural transformation lead to the conclusion that this process looks more like a phase transition of the second than of the first order. Whether this conclusion is really true, and maybe even universal for all of the thermotropic LC CPEs, has to be shown by further studies, which are in now progress.

Acknowledgements Financial support by the Deutsche Forschungsgemeinschaft and the Russian Foundation for Basic Research (grant no. 99-03-04003) as well as by the Foundation of the Russian Academy of Sciences for Young Scientists (grant no. 40) is gratefully acknowledged.

References

1. Brostow W, Hess M, Lopez BL (1994) Macromolecules 27:2262
2. Lu X, Windle AH (1995) Polymer 36:451
3. Windle AH, Viney C, Golombok R, Donald AM, Mitchell GR (1985) Faraday Discuss Chem Soc 79:55
4. Guttierezz GA, Chivers RA, Blackwell J, Stamatoff JB, Yoon H (1983) Polymer 24:937
5. Antipov EM, Godovsky YK, Stamm M, Fischer EW (1996) In: Isayev AI, Kyu T, Cheng SZD (eds)) Liquid-crystalline polymer systems. American Chemical Society, Washington, DC, pp 259–303
6. Antipov EM, Volegova IA, Godovsky YK (1994) Polym Sci Russ 36:1258
7. Antipov EM, Volegova IA, Godovsky YK (1995) Polym Sci Russ 37:523
8. Antipov EM, Volegova IA, Godovsky YK (1996) Vysokomolek Soedin 38:833
9. Antipov EM, Volegova IA, Godovsky YK, Stamm M, Fischer EW (1996) J Macromol Sci Phys 35:591
10. Hanna S, Romo-Uribe A, Windle AH (1993) Nature 366:546
11. Antipov EM, Volegova IA, Godovsky YK (1997) Vysokomolek Soedin 39:1791
12. Godovsky YK, Volegova IA (1994) Polym Sci Russ 36:342
13. Kudryavtseva SY (1996) Mech Compos Mater 32:98
14. Antipov EM, Stamm M, Fischer EW (1994) J Mater Sci 29:328
15. Vainshtein BK (1966) Diffraction of X-rays by chain molecules. Elsevier, Amsterdam
16. Wunderlich B, Möller M, Grebowitz J, Baur H (1988) Adv Polym Sci 87:1
17. Keller A, Ungar G (1991) J Appl Polym Sci 42:1683
18. Plate NA, Antipov EM, Kulichikhin VG (1992) Polym Sci Russ 34:498
19. Antipov EM, Podolsky YY, Stamm M, Fischer EW (1998) J Macromol Sci Phys 37:361